R. Linga Swamy, et. al. International Journal of Engineering Research and Applications
www.ijera.com
ISSN: 2248-9622, Vol. 11, Issue 10, (Series-IV) October 2021, pp. 21-28

RESEARCH ARTICLE OPEN ACCESS

Power Optimization of grid connected DFIG wind energy system

R. Linga Swamy
Assistant Professor, Department of Electrical Engineering, University college of Engineering, Osmania University Hyderabad, Telangana, India

E. Sreeshobha
Assistant Professor, Department of Electrical Engineering, University college of Engineering, Osmania University Hyderabad, Telangana, India

M. Rathan Pradeep
ME Student, Department of Electrical Engineering, University college of Engineering, Osmania University Hyderabad, Telangana, India

ABSTRACT
During the last decades, the concept of a variable-speed wind turbine (WT) has been receiving increasing attention. It is due to the fact that it is more controllable and efficient. As the demand of controllability of variable speed WTs increases, it is necessary to investigate the modelling of wind turbine-generator systems (WTGS) that are capable of accurately simulating the behavior of each component in the WTGS. This paper will provide the method of optimum power extraction from grid-connected doubly-fed induction generator (DFIG) wind energy system. In order to obtain satisfying output power from the WTGS, control strategies are to be developed. These control schemes include the stator-side converter control, the rotor-side converter control and the pitch angle control. The grid-side converter controller is used to keep the DC-link voltage constant. The generator-side converter controller has the ability of regulating the torque, active power and reactive power. The pitch angle control scheme is used to regulate the pitch angle and thus keep the output power at rated value even when the wind speed experiences gusts. Above stated control strategies for DFIG are developed in MATLAB/Simulink and simulated for three different winds namely constant wind, ramp wind and step wind inputs. Comparison of active powers with and without pitch angle control and reactive power control is made and tabulated.
Keywords— *DFIG, pitch angle control, reactive power control.*

Date of Submission: 18-10-2021 Date of Acceptance: 02-11-2021

I. INTRODUCTION

The increasing emphasis on renewable wind energy has given rise to augmented attention on more reliable and advantageous electrical generator systems. Induction generator systems have been widely used and studied in wind power system because of their advantages over synchronous generators, such as smaller size, lower cost, and lower requirement of maintenance. The straightforward power conversion technique using squirrel-cage induction generator (SCIG) is widely accepted in fixed-speed applications with less emphasis on the high efficiency and control of power flow. However, such direct connection with grid would allow the speed to vary in a very narrow range and thus limit the wind turbine utilization and power output. Another major problem with SCIG power system is the source of reactive power; that is, an external reactive power compensator is required to hold the distribution line voltage and prevent the whole system from overload. On the other hand, the doubly fed induction generator (DFIG) with variable-speed ability has higher energy capture efficiency and improved power quality and thus has attracted more attentions[1]-[6]. With the advent of power electronic techniques, a back-to-back converter, which consists of two bidirectional converters and a dc link, acts as an optimal operation tracking interface between generator and grid. Field-oriented control (FOC) is applied to both rotor- and stator-side converters to achieve desirable control on voltage and power. Generally, the FOC has been presented based on DFIG mathematical equations only [7]-[14]. However, a three-phase choke is

commonly used to couple the stator-side converter into the grid. Therefore, this paper investigates the FOC schemes of stator-side converter involving the choke, and it turns out that both stator- and rotor-side converter voltages consist of a current regulation part and a cross-coupling part.

The Field Orientated Control (FOC) consists of controlling the stator currents represented by a vector. This control is based on projections which transform a three phase time and speed dependent system into a two co-ordinate (d and q co-ordinates) time invariant system. These projections lead to a structure similar to that of a DC machine control. Field orientated controlled machines need two constants as input references: the torque component (aligned with the q co-ordinate) and the flux component (aligned with d co-ordinate). As Field Orientated Control is simply based on projections the control structure handles instantaneous electrical quantities. This makes the control accurate in every working operation (steady state and transient) and independent of the limited bandwidth mathematical model.

II. DOUBLY FED INDUCTION GENERATOR

A. Torque production in the DFIG

The DFIG consists of stator windings connected directly to the grid, and wound rotor windings connected to a power converter. Torque is created by the interaction of the rotor magnetic field with the stator magnetic field. The magnitude of the generated torque is dependent on strength of both the magnetic fields, and the angular displacement between the two. If the two magnets are placed orthogonal to each other, with the north and south poles 90 degrees displaced the generated torque the greatest.

As the stator is connected directly to the grid, the stator field is a function of the grid voltage, with a rotation based on the grid frequency and coinciding with the synchronous speed. The grid voltage can be assumed to be more or less constant and therefore the stator flux can be considered constant. The rotor flux is dependent on the rotor current, which is controlled directly by the power converter. Therefore, the torque production in the DFIG can be directly controlled by control of the rotor current magnitude and angular position relative to the stator flux. This is done by calculation of the angular position and magnitude of the stator flux by monitoring the applied stator voltage and controlling the rotor currents such that they are normal to the stator flux, at the magnitude required to generate the needed torque.

B. The rotor side converter (RSC)

The rotor side converter (RSC) is used to control the torque production of the DFIG through direct control of the rotor currents by applying a voltage to the rotor windings that corresponds to the desired current. The RSC will operate at varying frequencies corresponding to the variable rotor speed requirements based on the wind speed. This output power is controlled to follow the wind turbine's power-speed characteristic curve. In order to extract this power most efficiently, the optimal tip-speed ratio must be kept before rated power is reached, corresponding to a different rotor speed for each power level. The actual output power from the generator, plus all power losses, is compared to this reference power from the power-speed curve. A Proportional Integral (PI) controller is used to control the torque, speed, or power to its reference value. The output of the controller is the reference rotor current required to generate the desired torque or power. An inner PI control loop is then used to control the rotor current error to its reference value, with the rotor voltage reference as the controller output. The rotor current can also be used to control the reactive power production of the DFIG.

C. The Grid side converter (GSC)

The grid side converter is used to regulate the voltage of the DC link between the two converters. The GSC contains on outer loop control that controls the DC-link voltage, attempting to control it to nominal value. An inner PI control loop controls the GSC current. Commonly the GSC acts to set Qgc = 0 and maximize active power output. As the GSC is connected directly to the grid, output power is at a fixed frequency corresponding to the grid frequency.

D. Pitch Angle Control

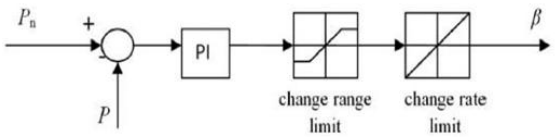

Fig.1. Pitch Angle control

The pitch angle control operates in such a way so as to make the pitch angle (β) =0 if the wind speed is less than nominal speed of 11m/s and β greater than zero for speeds greater than 11m/s such that the generated power does not cross the nominal power output.

III. CONTROL SCHEME FOR ROTOR AND STATOR SIDE CONVERTERS

The control system is divided into two parts stator-side converter control system and rotor-side converter control system. An equivalent circuit of DFIG is depicted in fig 2, and the relation equations

for voltage *V*, current *I*, flux Ψ, and torque *Te* involve are given in equations (1) to (9).

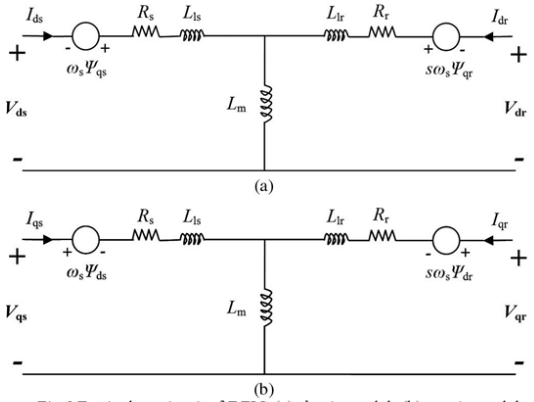

Fig.2 Equivalent circuit of DFIG (a) *d*-axis model. (b) *q*-axis model

$$V_{ds} = R_s I_{ds} - \omega_s \Psi_{qs} + \frac{d\Psi_{ds}}{dt} \quad (1)$$

$$V_{qs} = R_s I_{qs} + \omega_s \Psi_{ds} + \frac{d\Psi_{qs}}{dt} \quad (2)$$

$$V_{dr} = R_r I_{dr} - s\omega_s \Psi_{qr} + \frac{d\Psi_{dr}}{dt} \quad (3)$$

$$V_{qr} = R_r I_{qr} + s\omega_s \Psi_{dr} + \frac{d\Psi_{qr}}{dt} \quad (4)$$

$$\Psi_{ds} = L_s I_{ds} + L_m I_{dr} \quad (5)$$

$$\Psi_{qs} = L_s I_{qs} + L_m I_{qr} \quad (6)$$

$$\Psi_{dr} = L_r I_{dr} + L_m I_{ds} \quad (7)$$

$$\Psi_{qr} = L_r I_{qr} + L_m I_{qs} \quad (8)$$

$$T_e = \frac{3}{2} n_p (\Psi_{ds} I_{qs} - \Psi_{qs} I_{ds}) \quad (9)$$

where $Ls = Lls + Lm$; $Lr = Llr + Lm$; $s\omega s = \omega s - \omega r$ represents the difference between synchronous speed and rotor speed; subscripts *r*, *s*, *d*, and *q* denote the rotor, stator, *d*-axis, and *q*-axis components, respectively; Te is electromagnetic torque; and *Lm*, *np*, and *J* are generator mutual inductance, the number of pole pairs, and the inertia coefficient, respectively.

A. Rotor-side converter control

If the derivative parts in (1) and (2) are neglected, one can obtain stator flux as

$$\Psi_{ds} = (V_{qs} - R_s I_{qs})/\omega_s \quad (10)$$

$$\Psi_{qs} = (V_{ds} - R_s I_{ds})/(-\omega_s) \quad (11)$$

$$\Psi_s = \sqrt{{\Psi_{ds}}^2 + {\Psi_{qs}}^2} \quad (12)$$

Because of being directly connected to the grid, the stator voltage shares constant magnitude and frequency of the grid. One could make the d-axis align with stator voltage vector; it is true that Vs = Vds and Vqs = 0, thus Ψs = Ψqs and Ψds = 0, which is of stator-voltage-oriented vector control scheme.

$$I_{dr\_ref} = -\frac{2L_s T_e}{3n_p L_m \Psi_s} \quad (13)$$

Where

$$P_{e\_ref} = P_{opt} - P_{loss} = \quad (14)$$

$$P_{loss} = R_s {I_s}^2 + R_r {I_r}^2 + R_c {I_{sc}}^2 + F{\omega_r}^2 \quad (15)$$

where I_{sc}, *Rc*, and *F* are stator-side converter current, choke resistance, and friction factor, respectively. $P_{opt,} P_{e\_ref,}$ and $P_{loss,}$ are desired optimal output active power, reference active power, and system power loss. Combining (10)–(15), the active power is used as command inputs to determine current reference $I_{dr\_ref,}$. Meanwhile, the output reactive power is the stator reactive output power since the stator-side converter's reactive power is set to be zero

$$Q_0 = Q_s + Q_{sc} = Q_s = \boldsymbol{Im}\left[(V_{ds} + jV_{qs})(I_{ds} + jI_{qs})^*\right] \quad (16)$$

$$-V_{ds} I_{qs} = -V_{ds} \frac{1}{L_s} (\Psi_s - L_m I_{qr}) \quad (17)$$

Thus, the regulation of reactive power can lead to I_{qr_ref} and

then the rotor-side converter voltage signals ${V_{dr}}^1$ and ${V_{qr}}^1$ are derived by regulation of currents. In addition, the feed forward coupling part ${V_{dr}}^2$ and ${V_{qr}}^2$ are derived based on

$${V_{dr}}^2 = R_r I_{dr} - s\omega_s (L_r I_{qr} + L_m I_{qs}) \quad (18)$$

$${V_{qr}}^2 = R_r I_{qr} + s\omega_s (L_r I_{dr} + L_m I_{ds}) \quad (19)$$

Where, the superscripts 1 and 2 denote the current regulation part and cross-coupling part respectively. At last, rotor-side converter voltage signals in d/q-axis are expressed as:

$$V_{drc} = V_{dr} = V_{dr}{}^{1} + V_{dr}{}^{2} \quad (20)$$

$$V_{qrc} = V_{qr} = V_{qr}{}^{1} + V_{qr}{}^{2} \quad (21)$$

Where subscript rc denotes the rotor-side converter. After
the conversion of dq-abc, the rotor-side converter voltage $V_{abc\_rc,}$ can be obtained. Fig.10 exhibits the control scheme for above procedure.

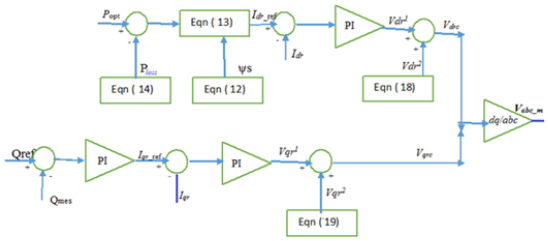

Fig.3. Rotor side control

B. Stator-side converter control

Concerning of the use of three-phase series *RL* choke between stator and stator-side converter, a cross-coupling model is required to derive the voltage signal of stator-side converter.

$$V_{dsc} = V_{ds} - V_{dch} \quad (22)$$

$$V_{qsc} = V_{qs} - V_{qch} \quad (23)$$

Where the subscript sc and ch denote the variables of stator side converter and choke. The coupling part of voltage signals $V_{dch}{}^{2}$ and $V_{qch}{}^{2}$

$$V_{dch}{}^{2} = R_c I_{dsc} - \omega_s L_c I_{qsc} \quad (24)$$

$$V_{qch}{}^{2} = R_c I_{qsc} + \omega_s L_c I_{dsc} \quad (25)$$

Besides, $V_{dch}{}^{1}$ and $V_{qch}{}^{1}$ are determined by regulation of current I_{dsc} and I_{qsc} in which the current reference $I_{qsc\_ref,}$ is given directly while $I_{dsc\_ref,}$ is determined by the regulation of dc-link voltage V_{dc}. Thus, above all, the stator-side converter voltage signals V_{dsc} and V_{qsc} are obtained as following and depicted in

$$V_{dsc} = V_{ds} - V_{dch}{}^{1} - V_{dch}{}^{2} \quad (26)$$

$$V_{qsc} = V_{qs} - V_{qch}{}^{1} - V_{qch}{}^{2} \quad (27)$$

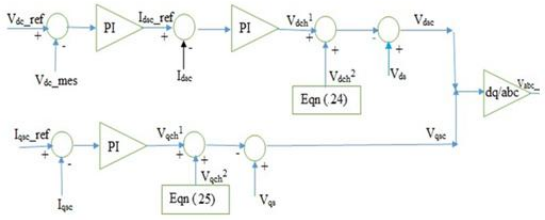

Fig.4.Stator side control

IV. SIMULATION

Fig.5 shows the main simulation diagram where the sub-system (consisting of DFIG) is connected to grid through transformers and transmission line. Programmable voltage source is considered as grid where the grid voltage is 120kV.

A control is developed to generate gating pluses to back to back converters which is simulated as follows. Two differently developed models are separately used to generate gating pulses for both stator as well as rotor side converters as shown in Fig.6 and Fig.7 because stator side converter is used to control the DC-link voltage between converters where as rotor side converter uses a speed controller or torque controller to regulate output power and it also maintains the reactive power of system at zero. both controls finally gives out the required reference voltage that is compared with carrier waveform using PWM generator to give out gate pulses. Fig.8 shows the simulation diagram of Reactive power control.

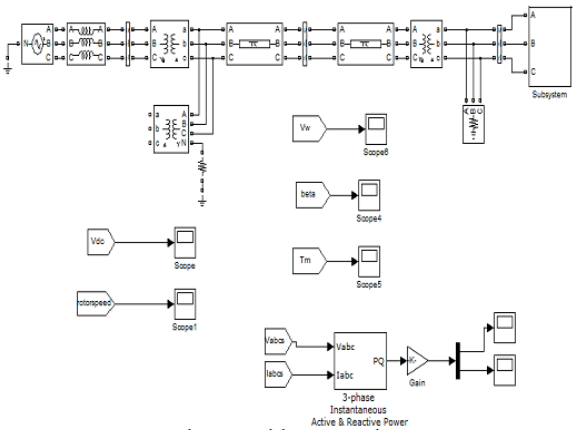

Fig.5. Grid connection

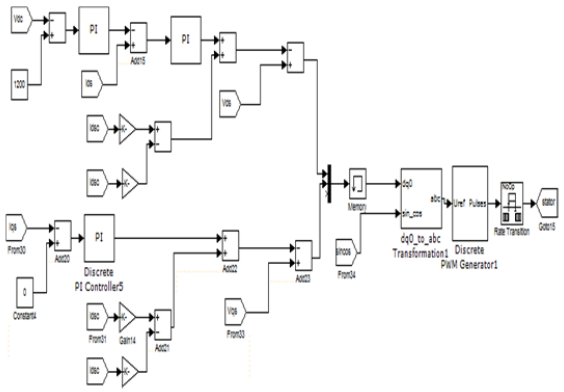

Fig.6 Stator Side Converter Control

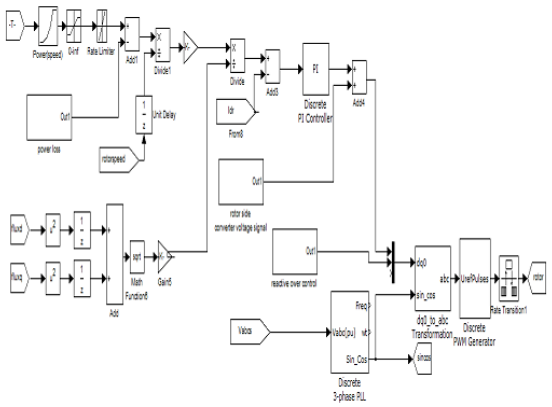

Fig.7 Rotor Side Converter Control

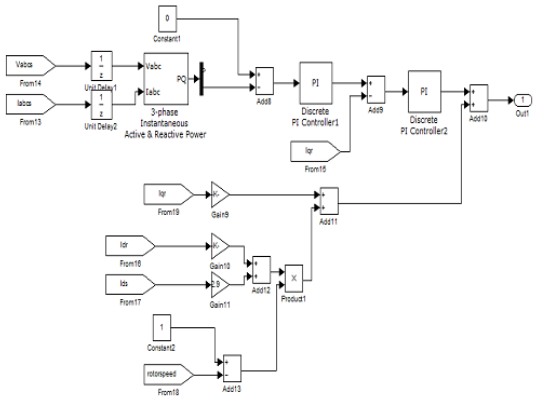

Fig.8 Reactive Power Control

Fig.9 shows model of pitch angle control where rated power is compared with generated power and error minimized using PI-controller and the generated pitch angle is fed to turbine input.

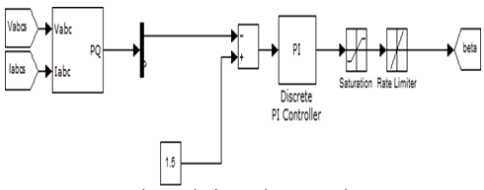

Fig.9 pitch angle control

V. SIMULATION RESULTS

MATLAB model has been simulated for three types of winds namely constant wind, ramp type of wind and step wind inputs.

A. Contant wind speed (7m/s)

By using the proposed optimal power curve as well as the system parameters, the DFIG wind power system is simulated. The independent control of active and reactive power is achieved as shown in Fig. 10 and 11. At constant input wind speed of v_w = 7 m/s, the optimal output active power is 0.255MW with nominal power of 1.5 MW. Fluctuations in power initially, observed from simulation results are due to power loss. The optimal rotor speed is also achieved at 0.75 p.u. and the DC-link voltage is 1200V maintained at nominal value.

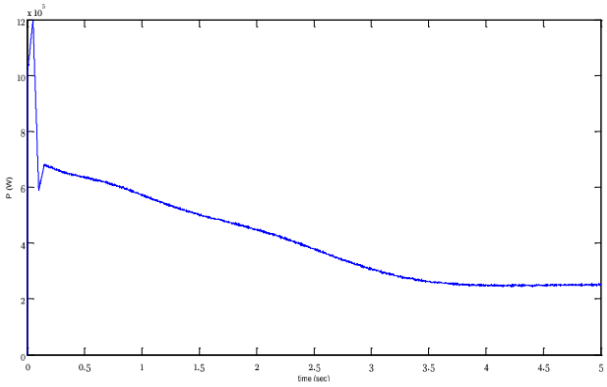

Fig.10 Active Power

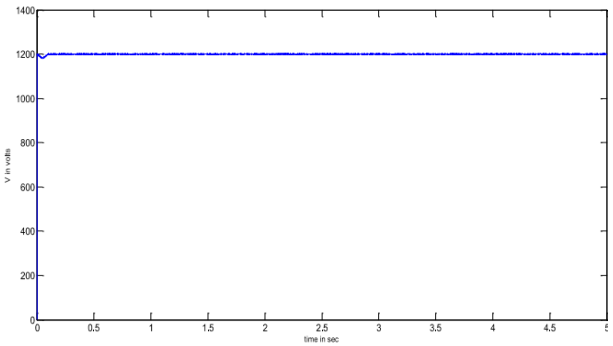

Fig.11. Reactive Power

B. Ramp Type wind speed

The behaviour of DFIG is analyzed for ramp input wind speed which varies in amplitude from initial value 8m/s to final value 12m/s at t=0.1. We observe the following waveform of Fig. 12 and 13 having voltage at 1200V, active power observed is 0.7MW. Initially for 8m/s speed the curve shoes behaviour of constant wind (under rated) and later active power rises.

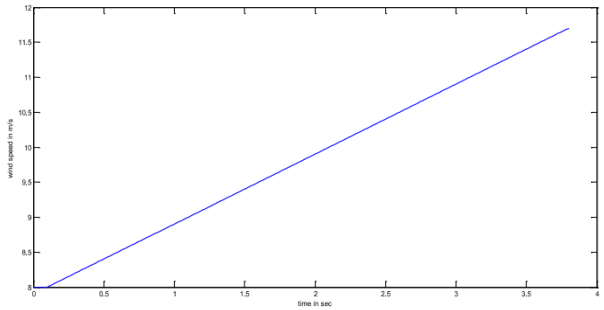

Fig.12. Wind Speed Ramp (8m/s to 12m/s)

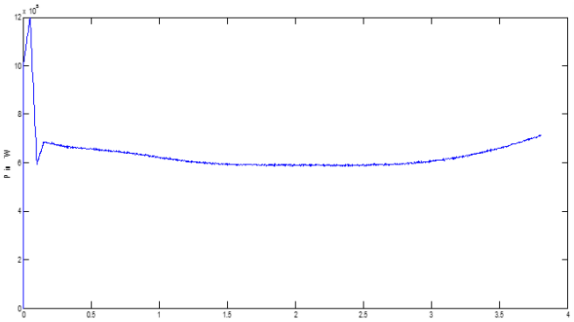

Fig.13. Active Power

C. Step input of wind

From Fig. 14 and 15 it is observed that wind speed is maintained at 4m/s from 0 to 0.1ec. From 0.1 to 1sec, speed of the wind is maintained at 7m/s which is below rated value. At 1sec, there is a step rise in amplitude to 13m/s. As a result, an increase in active power from 1sec occurs. This is due to pitch angle control that limits active power below rated value even for above rated wind speeds. The DC-link voltage remains at 1200V and reactive power settles to zero, rotor speed also increases with input wind speed is 1.25p.u.

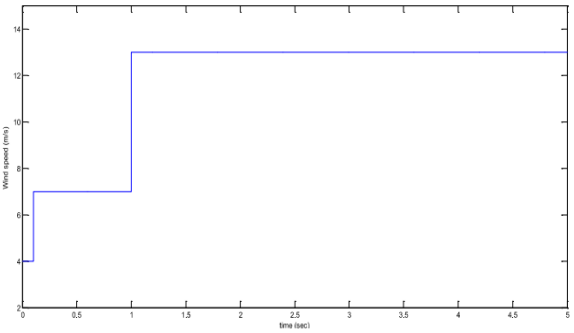

Fig.14. Step type wind speed

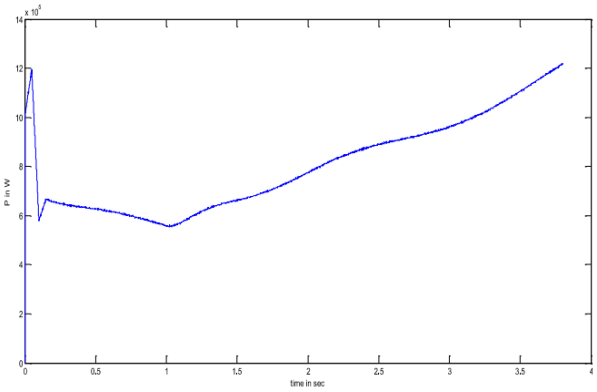

Fig.15. Active power

The Tabulation for 3 different cases of wind speeds is shown in this chapter i) 7m/s ii) 14m/s iii) Ramp wind speed 7m/s-14m/s. As the nominal speed is taken as 11m/s the pitch angle control makes the pitch angle (β)=0 for wind speeds less than 11m/s and for wind speeds greater than 11m/s the pitch angle (β) will be made greater than zero such that the generated power does not go greater than the nominal power or the power handling capacity of the DFIG system.

Thus, the pitch angle control prevents the output power from exceeding the nominal value and will be stabilized at nominal value where the wind speed is above the nominal speed.

The output active and reactive power is compared in two cases i) with and without pitch angle control ii) with and without reactive power control

D. Tabulation for constant wind speed 7m/s

For wind speed at 7m/s the pitch angle (β) is taken as 0º as the speed is less than the nominal wind speed of 11m/s and the reactive power control makes the output reactive power closer to zero

TableI. Power with Pitch angle and Reactive Power Control

Power with Pitch angle control (Beta=0)	
Active Power (MW)	Reactive Power (VAR)
0.255MW	15.95

TableII. Power without pitch angle control

Active Power without pitch angle control	
Pitch angle (β)	Active Power (MW)
0	0.255
5	0.122
10	0.056
25	0
45	0

The Reactive power is significantly higher when there is no reactive power control resulting in lesser active power output and losses resulting in over heating of the DFIG system

Table III. Reactive Power with no pitch angle control

With Reactive power control			Without Reactive Power control	
Pitch angle (β)	Active Power (MW)	Reactive Power (VAR)	Active Power (MW)	Reactive Power (VAR)
0	0.255	15.95	0.215	8534
5	0.122	3.21	0.104	5687
10	0.056	0.45	0.041	1890
25	0	0.32	0	0.56
45	0	0.3	0	0.23

E. Tabulation for constant wind speed of 14m/s

For wind speed at 14m/s the pitch angle (β) is taken as 12º as the speed is more than the nominal wind speed of 11m/s. The active power is controlled by pitch angle control so as not to cross the nominal power of 1.5MW. The reactive power control makes the output reactive power closer to zero.

TableI V. Active Power with pitch angle control

Power with Pitch angle control (Beta=12)	
Active Power (MW)	Reactive Power (VAR)
1.42	66.95

The following table illustrates the possible power output at 14m/s wind speed when there is no pitch angle control. At β=0 the power is significantly higher than the nominal power and decreases as the pitch angle is increased.

TableV. Active Power without Pitch angle control

Active Power without pitch angle control	
Pitch angle (β)	Active Power (MW)
0	1.95
5	1.71
12	1.46
25	0.89
45	0.21

The following table illustrates the comparison between active and reactive powers with and without reactive power control at different pitch angles.

Table VI. Reactive power without pitch angle control

With Reactive power control			Without Reactive Power control	
Pitch angle (β)	Active Power (MW)	Reactive Power (VAR)	Active Power (MW)	Reactive Power (VAR)
0	1.95	138.3	1.78	63686
5	1.71	98.62	1.57	55856
10	1.63	79.44	1.44	51701
25	0.89	43.14	0.77	44631
45	0.21	14.02	0.16	13601

F. Tabulation for wind speed- ramp(7m/s-4m/s)

Table VII. Power with pitch angle control for ramp wind speed

Power with pitch angle control (7-11)β=0, (11-14)β>0		
Wind Speed (m/s)	Pitch angle(β)	Active Power (MW)
7	0	0.255
9	0	0.642
11	2	1.39
13	8	1.41
14	12	1.42

Table VIII. Wind speed (m/s)

Active Power without pitch angle control		
Wind Speed (m/s)	Pitch angle (β)	Active Power (MW)
7	0	0.255
9	0	0.652
11	0	1.37
13	0	1.63
14	0	1.95

Table IX. Comparison between power with and without pitch angle control

Power with pitch angle control (7-11)β=0, (11-14)β>0			Power without pitch angle control	
Wind Speed (m/s)	Pitch angle(β)	Active Power (MW)	Pitch angle (β)	Active Power (MW)
7	0	0.255	0	0.255
9	0	0.642	0	0.652
11	2	1.39	0	1.37
13	8	1.41	0	1.63
14	12	1.42	0	1.95

Table X. Com Reactive power control comparison with pitch angle control at different wind speeds

With Reactive power control				Without Reactive Power control	
Wind Speed (m/s)	Pitch angle(β)	Active Power (MW)	Reactive Power (VAR)	Active Power (MW)	Reactive Power (VAR)
7	0	0.255	15.94	0.216	8456
9	0	0.642	63.36	0.525	26511
11	2	1.39	126.56	1.31	42475
13	8	1.41	145.28	1.31	43958
14	12	1.42	171.02	1.32	46398

VI. CONCLUSION

In this paper, control of a doubly-fed induction generator based wind energy system is analyzed, more specifically, the modeling of different components, the control strategies for the back-to-back converter. The model of a wind turbine-generator system equipped with a doubly-fed induction generator is developed and simulated in a MATLAB/Simulink environment. The gird-side converter control, generator-side converter control, and pitch angle control has been implemented. It is observed that the DC-link voltage is maintained constant regardless of the magnitudes of the grid voltages, and to yield a unity power factor looking in to the WTGS from the grid-side. The fitting curve considered provides the reference value of stator active power for the generator-side converter control. The pitch angle control regulates the pitch angle when the captured wind power exceeds its rated value or the wind speed exceeds its rated value. With these control schemes, the wind turbine is capable of providing satisfactory performances under various wind speed conditions.

REFERENCES

[1]. Yu Zou, Malik E. Elbuluk "Simulation Comparisons and Implementation of Induction Generator Wind Power Systems" IEEE Transactions on Industry Applications

[2]. 2. Raymond W. Flumerfelt and Su Su Wang, "Wind turbines," in AccessScience McGraw-Hill Companies, 2009, http://www.accessscience.com.

[3]. Bijaya Pokharel, "Modeling, Control and Analysis of a Doubly Fed Induction Generator Based Wind Turbine System with Voltage Regulation", Tennessee Technological University, Master thesis, December 2011.

[4]. Xin Jing "Modeling and Control of A Doubly-Fed Induction Generator For Wind Turbine-Generator Systems "Marquette University, Master's Thesis (2009).

[5]. H. Sun, Y. Ren, and H. Li, "DFIG wind power generation based on back-to-back PWM converter," in Proc. IEEE Int. C on f. Mechatron. Autom.,Aug. 2009, pp. 2276–2280.

[6]. L. Xu and P. Cartwright, "Direct active and reactive power control of DFIG for wind energy generation," IEEE Trans. Energy Convers., vol. 21, no. 3, pp. 750–758, Sep. 2006.

[7]. Vigneshwaran Rajasekaran "Modelling, Simulation and Development of Supervision Control System For Hybrid Wind Diesel System"

[8]. R. W. Righter, Wind Energy in America: A History, University of Oklahoma Press, 1996.

[9]. A.M. Bobely and J. F. Kreider, "Distributed Generation: The Power Paradigm for the New Millennium", CRC Press LLC, 2001.

[10]. M. Jaccard, "Renewable Portfolio Standard," Encyclopedia of Energy, Elsevier, vol. 5, pp. 413-421, 2004.

[11]. H. Li, Z. Chen and J. K. Pedersen, "Optimal Power Control Strategy of Maximizing Wind Energy Tracking and Conversion for VSCF Doubly Fed Induction Generator System,"in CES/IEEE 5th International Power Electronics and Motion Control Conference (IPEMC),2006.

[12]. M. Singh and S. Santoso, "Dynamic Models for Wind Turbines and Wind Power Plants," NREL, 2011.

[13]. Nasir Abdulai Boakye-Boateng, "Real-Time Simulation Of A Doubly-Fed Induction Generator Based Wind Power System On Emegasim® Real-Time Digital Simulator"

[14]. S. Mathew, "Wind Energy: Fundamentals, Resource Analysis and Economics", Netherlands: Springer, 2006.